International Journal of Nanomedicine

Dovepress
open access to scientific and medical research

Open Access Full Text Article

ORIGINAL RESEARCH

Intravesical delivery of rapamycin via folate-modified liposomes dispersed in thermo-reversible hydrogel

This article was published in the following Dove Press journal:
International Journal of Nanomedicine

Ho Yub Yoon[1,*]
In Ho Chang[2,*]
Yoon Tae Goo[1]
Chang Hyun Kim[1]
Tae Hoon Kang[1]
Soo-Yeon Kim[3]
Sang Jin Lee[3]
Seh Hyon Song[4]
Young Mi Whang[2]
Young Wook Choi[1]

[1]College of Pharmacy, Chung-ang University, Seoul, Korea; [2]College of Medicine, Chung-ang University, Seoul, Korea; [3]Research Institute, National Cancer Center, Goyang, Korea; [4]College of Pharmacy, Kyungsung University, Busan, Korea

*These authors contributed equally to this work

Purpose: To develop an intravesical instillation system for the treatment of bladder cancer, rapamycin (Rap) was encapsulated into liposomes and then homogeneously dispersed throughout a poloxamer 407 (P407)-based hydrogel.

Methods: Rap-loaded conventional liposomes (R-CL) and folate-modified liposomes (R-FL) were prepared using a film hydration method and pre-loading technique, and characterized by particle size, drug entrapment efficiency, and drug loading. The cellular uptake behavior in folate receptor-expressing bladder cancer cells was observed by flow cytometry and confocal laser scanning microscopy using a fluorescent probe. In vitro cytotoxic effects were evaluated using MTT assay, colony forming assay, and Western blot. For in vivo intravesical instillation, Rap-loaded liposomes were dispersed in P407-gel, generating R-CL/P407 and R-FL/P407. Gel-forming capacities and drug release were evaluated. Using the MBT2/Luc orthotopic bladder cancer mouse model, in vivo antitumor efficacy was evaluated according to regions of interest (ROI) measurement.

Results: R-CL and R-FL were successfully prepared, at approximately <160 nm, 42% entrapment efficiency, and 57 μg/mg drug loading. FL cellular uptake was enhanced over 2-fold than that of CL; folate receptor-mediated endocytosis was confirmed using a competitive assay with folic acid pretreatment. In vitro cytotoxic effects increased dose-dependently. Rap-loaded liposomes inhibited mTOR signaling and induced autophagy in urothelial carcinoma cells. With gelation time of <30 seconds and gel duration of >12 hrs, both R-CL/P407 and R-FL/P407 preparations transformed into gel immediately after instillation into the mouse bladder. Drug release from the liposomal gel was erosion controlled. In orthotopic bladder cancer mouse model, statistically significant differences in ROI values were found between R-CL/P407 and R-FL/P407 groups at day 11 (P=0.0273) and day 14 (P=0.0088), indicating the highest tumor growth inhibition by R-FL/P407.

Conclusion: Intravesical instillation of R-FL/P407 might represent a good candidate for bladder cancer treatment, owing to its enhanced retention and FR-targeting.

Keywords: bladder cancer, prolonged retention, enhanced uptake, antitumor efficacy, autophagy, mTOR signaling

Correspondence: Young Wook Choi
College of Pharmacy, Chung-Ang University, 84 Heukseok-ro, Dongjak-gu, Seoul 06974, Korea
Tel +82 2 820 5609
Fax +82 2 826 3781
Email ywchoi@cau.ac.kr

Young Mi Whang
College of Medicine, Chung-Ang University, 84 Heuksuk-Ro, Dongjak-gu, Seoul 06974, Korea
Tel +82 102 077 9024
Email ymwhang@gmail.com

Introduction

Bladder cancer accounts for approximately 90% of cancers of the urinary tract and is one of the most common cancers in both men and women.[1] Bladder urothelial cell carcinomas generally consist of a superficial disease termed non-muscle-invasive bladder cancer, with the treatment and prognosis normally dependent on how deep the bladder cancer has invaded.[2] The standard therapy comprises a combination of transurethral resection and intravesical instillation of chemotherapeutic agents.[3] In particular, mitomycin C has been used to decrease the risk of

recurrence[4] and doxorubicin and/or paclitaxel can be used as a drug of second choice depending on the response to the treatments.[5] However, in clinical practice, intravesical immunotherapy with Bacillus Calmette-Guérin, an application unique among cancer therapeutics, represents the most effective treatment to reduce disease progression and rate of recurrence.[6]

Rapamycin (Rap), a macrocylic lactone first discovered as a product of the soil bacteria *Streptomyces hygroscopicus*, has been used as an immune-suppressant to prevent rejection in organ transplantation.[7] Recently, a potent antitumor activity of Rap in a variety of solid tumors has been reported.[8–10] Intravesical administration of Rap was highly effective for suppressing bladder tumorigenesis,[11] supporting its potential as a chemotherapeutic agent for bladder cancer therapy. However, because of its poor water solubility, the therapeutic application of Rap and development of effective dosage forms have been very limited.[12] In addition, the presence of the luminal urothelial surface covered by a continuous mucin layer in the bladder is a crucial factor that prevents the adhesion of foreign substances and limits the absorption or penetration of instilled drugs.[13]

To overcome these obstacles, nanoparticulate carrier systems including liposomes have been widely utilized[3] with numerous studies having reported the use of liposomes as a vehicle for anticancer drugs for the treatment of bladder cancer and urinary tract disorders.[14–16] Moreover, liposomal nanocarriers can be further surface-modified for targeted drug delivery. Various ligands including specific small molecules and antibodies have been widely introduced for selective binding of the carriers to the target cells.[17] Specifically, folate has been extensively used as a targeting molecule to the folate receptor (FR), which is highly overexpressed in most malignant tumors of epithelial origin.[18] The high affinity to FR consequently results an increased cellular uptake, as FR recognition facilitates the delivery of folate-tethered substances via receptor-mediated endocytosis.[19,20] Thus, FR-targeting strategies impart substantial beneficial impact on the treatment of FR-expressing cancer cells.

Intravesical drug delivery permits the direct administration of therapeutic agents into the bladder via insertion of a urethral catheter,[21] thereby affording minimized systemic effects and improved exposure of the diseased tissues to therapeutic agents. Moreover, as the urothelial layer of the bladder is not vascularized, systemic administration of drug is undesirable.[22] Previously, to extend drug residence in the bladder, we had developed a thermo-sensitive hydrogel formulation using poloxamer 407 (P407),[23] a well-recognized temperature-sensitive polymer approved by the United States Food and Drug Administration as being non-toxic. Owing to its thermoreversible properties, P407 can remain in a free-flowing solution at low temperature (<21 °C) but forms a gel inside the bladder consequent to the elevated body temperature. This thermo-sensitive hydrogel has been extensively reported to serve as a depot on the bladder wall,[24,25] offering enhanced residence time in the bladder with continuous release of drugs. Moreover, numerous literatures dealt with the therapeutically beneficial use of hydrogels in terms of time-controlled drug delivery.[26–28]

In the present study, Rap-loaded liposomal hydrogels were fabricated, in which Rap was encapsulated into liposomes and homogeneously dispersed throughout the P407-based hydrogels. The respective systems comprised either Rap-loaded conventional liposomes (R-CL) or Rap-loaded folate-modified liposomes (R-FL) within a polymeric network of P407 hydrogel, designated as R-CL/P407 or R-FL/P407, respectively. These systems were characterized with regards to both in vitro properties such as cell uptake, cytotoxicity, and drug release, along with in vivo antitumor efficacies in an orthotopic mouse cancer model. As postulated in Figure 1, intravesical instillation of R-FL/P407, R-FL continuously released from the hydrogel matrix in an erosion-controlled manner, followed by FR-mediated endocytosis, thus enhancing target cell apoptosis through autophagy induced by Rap.

Materials and methods

Materials

Rap (purity >99%) was kindly provided by Chong Kun Dang Pharm. Co. (Yongin, Korea). Soy phosphatidylcholine (SPC; purity >99%) and distearoylphosphatidylethanolamine-polyethylene glycol$_{2000}$-folate (DSPE-PEG$_{2000}$-Fol; DP$_{2K}$F) were purchased from Avanti® Polar Lipids (Alabaster, AL, USA). 1,1′-dioctadecyl-3,3,3′,3′-tetramethylindocarbocyanine perchlorate (DiI), phosphate buffered saline (PBS) tablets, and cholesterol were purchased from Sigma-Aldrich (St. Louis, MO, USA). Folic acid was purchased from Duksan Pure Chemical Co., Ltd. (Seoul, Korea). Acetonitrile, chloroform, dimethylsulfoxide, and other solvents purchased from commercial sources were of analytical or cell culture grade. The following antibodies were purchased from Cell Signaling Technology (Danvers,

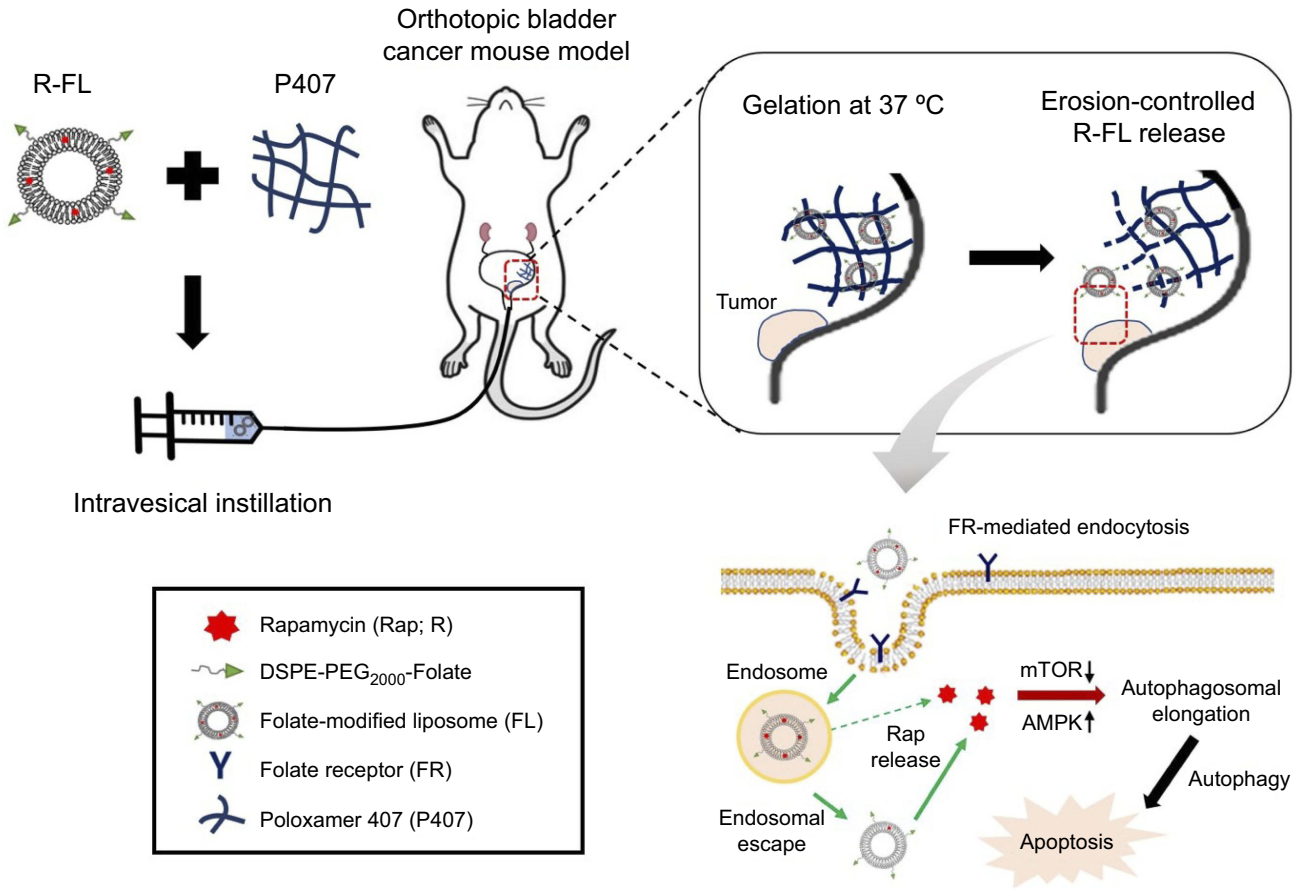

Figure 1 Schematic representation of intravesical instillation of R-FL/P407, followed by gelation in the bladder, erosion-controlled R-FL release, and enhanced absorption via FR-mediated endocytosis.
Abbreviations: R-FL, rapamycin-loaded folate-modified liposome; P407, poloxamer 407; $DP_{2K}F$, distearoylphosphatidylethanolamine-polyethylene $glycol_{2000}$-folate; FR, folate receptor.

MA, USA): rabbit polyclonal antibodies against phosphorylated AMPKα (Thr172), phosphorylated mTOR (Ser2448), phosphorylated 4EBP-1, phosphorylated p70S6 (Ser371), phosphorylated ULK1 (Ser555 and Ser757), and cleaved PARP. Mouse monoclonal antibody against β-actin was purchased from Santa Cruz Biotechnology (Dallas, TX, USA). Rabbit polyclonal antibodies against LC3B, p62, and beclin-1 were purchased from Abcam (Cambridge, MA, USA).

Preparation of liposomal samples

A thin lipid film hydration method was used to prepare all liposomal vesicles.[29] Briefly, to prepare R-FL, SPC and cholesterol (9:1 molar ratio) were dissolved in a mixture of methanol and chloroform (2:1 v/v) in a round-bottomed flask, and $DP_{2K}F$ was added at 0.01–1% of the liposomal constituents, then Rap was dissolved (1 mg/mL) in the mixture using a pre-loading technique.[30] The organic solvent was then removed via rotary vacuum evaporation, followed by application of a nitrogen gas stream for 1 hr to remove the solvent traces. The thin lipid film was hydrated with 10 mM PBS (pH 7.4). The liposomal solution was then extruded with a mini-Extruder (Avanti® Polar Lipids), using 10 passes through a 200 nm polyethersulfone membrane to obtain homogenous size distributions. R-CL was prepared by the same procedure, excluding the addition of $DP_{2K}F$. To observe the cellular uptake of liposomes, DiI (a lipophilic red fluorescent probe) was loaded instead of Rap at a concentration of 100 μg/mL. The unencapsulated Rap or DiI was purified by ultra-centrifugation at 14,000 g for 15 min using Amicon® ultra-centrifugal filters (molecular weight cut off 100 kDa, Millipore, Billerica, MA, USA). Empty liposomes (CL and FL) were prepared without the addition of Rap or DiI. All prepared samples were filtered through a 0.2 μm syringe filter to maintain sterility for in vitro and in vivo experiments, then stored at 4 °C until use.

Particle size and zeta potential (ZP) analysis

Liposomal stock solutions were diluted with distilled water and examined for size distribution and polydispersity index (PDI) using a dynamic light scattering particle size analyzer (Zetasizer Nano-ZS; Marlvern Instruments, Worcestershire, UK) equipped with a 50-mV laser at a scattering angle of 90°. ZP measurements were obtained using disposable capillary cells and the M3-PALS measurement technology that accompanied the Zetasizer system.

High performance liquid chromatography (HPLC) assay of Rap and DiI

Quantitative determination of Rap was performed by using an HPLC system consisting of separations modules (Waters® e2695), a UV detector (Waters® e2489), and a data station (Empower® 3), which were purchased from Waters® Corporation (Milford, MA, USA). Rap was separated by using a C18 Column (Kromasil®, 5 μm, 4.6×250 mm; Akzo Nobel, Bohus, Sweden) with acetonitrile and water (75:25, v/v) as a mobile phase delivered at a flow rate of 1 mL/min. The column temperature was set to 40 °C.[31] Rap was detected at 277 nm, with an injection volume of 50 μL. The amount of DiI was separately quantified by using the same HPLC system with a fluorescence detector (Waters® W2475). Chromatography was carried out on a C18 Column (Shiseido, Tokyo, Japan) with 0.05 M dimethyl sulfate and methanol (2:98, v/v) as a mobile phase. The excitation and emission wavelengths were set at 549 and 565 nm, respectively.

Determination of entrapment efficiency (EE) and drug loading (DL)

The EE and DL of Rap or DiI in liposomal samples were determined via ultra-filtration, using Amicon® ultra-centrifugal filters. Briefly, an aliquot of the suspension was added to the sample reservoir and centrifuged for 15 min at 14,000 g to determine the concentration of free drug in the filtrate. The following equations were used for the calculations:

$$\text{EE } (\%) = \frac{W_T - W_F}{W_T} \times 100$$

$$\text{DL}(\mu g/mg) = \frac{W_T - W_F}{W_L}$$

where W_T, W_F, and W_L represent the total amount of the drug, the free amount of the drug, and the total amount of lipid, respectively.

Colloidal stability of liposomes

To evaluate the colloidal stability, liposomal samples were stored at 4 °C and 25 °C for one month. Aliquots were withdrawn periodically and subjected to particle size and ZP determination using dynamic light scattering. The percentage of initial drug loading was assessed using HPLC as described above.

Transmission electron microscopy

The morphology of R-L and R-FL was examined by using a transmission electron microscope (JEM1010; JEOL, Tokyo, Japan) operating at an acceleration voltage of 80 kV. Prior to staining, samples were diluted 1,000-fold by using distilled water and deposited onto the carbon-coated copper grid. A drop of 2% uranyl acetate solution was then applied to stain the samples. After washing with distilled water and drying at 25 °C, the replica on the grid was prepared on a sample holder and then subjected to examination under transmission electron microscopy.

Cell culture

Human 5637, and HT1376 urothelial carcinoma (URCa) cells were purchased from the American Type Culture Collection (Manassas, VA, USA). MBT2 mouse bladder cancer cells were purchased from the Korean Cell Line Bank (Seoul, Korea). All cells were maintained in RPMI 1640 medium supplemented with 10% fetal bovine serum (GIBCO-BRL, Gaithersburg, MD, USA) and penicillin/spectromycin in a humidified atmosphere using a 5% CO_2 incubator (Thermo Scientific, Waltham, MA, USA). The cells were sub-cultured every 3–5 days and used for experiments at passages 5–20.

Flow cytometry

The intracellular uptake behavior of CL and FL in 5637, HT1376, and MBT2 cells was investigated quantitatively by determining the mean fluorescence intensity (MFI) of DiI by flow cytometry using a FACSCalibur (Becton Dickinson, Bedford, MA, USA). Briefly, the cells were seeded into six-well plates at a density of 5×10^5 cells per well. After 24 hrs of incubation, the medium was removed and replaced with fresh medium after the cells were washed twice with PBS. Then, the cells were incubated

for 2 hrs at 37 °C in medium (2 mL) with CL and FL containing equivalent amounts of DiI (100 ng). Subsequently, the cells were washed twice with PBS, harvested using trypsin-EDTA, and suspended in PBS (1 mL). The cell suspensions were introduced into the flow cytometer. Cell-associated fluorescence was quantitatively determined by counting 10^4 events detected in the FL2 channel. Only the viable cells were gated for fluorescence analysis. Separately, to examine the role of folate binding on liposomal uptake, a competitive binding assay was performed with FL as previously reported.[20] Briefly, 1 mM of free folic acid was added to the medium in the FR blocking group 30 mins prior to the treatment. Following incubation for 2 hrs at 37 °C, cells were then washed two times with PBS to remove excess FA and unbound liposomes. The subsequent steps were performed using the same procedure as described above. All experiments were performed in triplicate.

Confocal laser scanning microscopy (CLSM)

To observe the time-dependent intracellular translocation of FL, CLSM was performed.[20] Briefly, cells were seeded in chambered glass slides (Thermo Scientific Nunc) at a density of 5×10^4 cells per well and incubated for 24 hrs at 37 °C. After 24 hrs, the cells were washed twice with PBS, which was then replaced with fresh medium containing FL, in which the concentration of DiI was 100 ng/mL. Following incubation, the cells were washed twice with PBS and fixed with 4% formaldehyde in PBS for 15 mins at room temperature. The cells were mounted by using Vectashield mounting medium containing DAPI (H-1200) to stain the nuclei and avoid fading. Finally, the cells were observed by using a confocal laser scanning microscope (Zeiss LSM 700 Meta confocal microscope; Carl Zeiss Meditec AG, Jena, Germany) under 400× magnification.

Cell viability assay

The in vitro cytotoxicity of various Rap formulations was analyzed using the 3-(4,5-dimethylthiazol-2-yl)-2,5-diphenyltetrazolium bromide (MTT) assay and colony-forming ability as previously reported.[32] Cells were treated with Rap, R-CL, or R-FL at various concentrations and incubated for 24, 48, and 72 hrs. Cell viability was measured using a microplate reader and calculated as the percentage of viable cells relative to untreated controls. The cytotoxicity of empty liposomal formulations was also evaluated using the same procedure. To assess their colony formation ability, cells were re-plated after 3 days in 12 well plates at a low density (5×10^2 cells per well) in complete medium for 2 weeks. The medium was replaced with fresh complete culture medium every 3 days. Colonies were fixed with ice-cold methanol and stained with crystal violet (0.1%; Sigma-Aldrich). Colony numbers were counted visually and colonies measuring at least 50 μm were counted.

Western blot analysis

After treatment with Rap, R-CL, or R-FL for 6 or 12 hrs, the cells were lysed and the total cell lysates subjected to sodium dodecyl sulfate-polyacrylamide gel electrophoresis (SDS-PAGE) as described previously.[33] Equal amounts of protein samples (20 μg/lane) were separated on 8% or 15% SDS-PAGE gels and then transferred onto polyvinylidene difluoride membranes (Millipore, Burlington, MA, USA). The membranes were blocked with Tris-buffered saline and 0.1% Tween 20 (TBS-T) containing 5% skim milk, and incubated with the primary antibodies overnight at 4 °C. The membrane was washed three times with TBS-T, following which the secondary antibody (1:5000) was added and the membrane was incubated for 1 hr at room temperature. The protein bands were visualized using an enhanced chemiluminescence solution (Bio-Rad, Hercules, CA, USA) and detected with a ChemiDoc gel imaging system (Bio-Rad). All experiments were performed in triplicate.

Preparation of the liposomal gel

The "cold method" was adopted to prepare the P407 hydrogel vehicle.[23,34] Briefly, an exact amount of P407 granules (2 g) was added to PBS solution (10 mL) in flat-bottomed screw-capped glass vials and gently mixed with magnetic stirrers for 24 hrs at 4 °C until all the pluronic granules were completely dissolved and a clear solution was obtained. Then, the R-CL and R-FL dispersions were added to the above 20% (w/w) P407 solutions to generate a final Rap concentration equal to 0.4 mg/mL. The mixture was stirred for another 24 hrs at 4 °C for homogenous dispersion, then stored in a refrigerator until use.

Characterization of the liposomal gel

The sol–gel transition characteristics of the liposomal gel were determined using the test-tube inversion method as previously reported.[23] Briefly, a 5 mL test tube containing 1 mL of sample was placed in a water-bath and heated slowly from 4 °C to 37 °C at a rate of 1 °C/min. At each temperature point, the flowability was observed by gently tilting the test tube. The temperature at which the sample did not flow for 30 seconds was determined as the gelation

temperature (G-Temp). The gelation time (G-Time) of the samples was similarly determined at 37 °C in a water-bath. The samples were placed into a test tube at a constant temperature of 37 °C and the tubes were inverted every 5 seconds. The time at which the samples did not flow for 30 seconds was recorded as the G-time. Separately, the gel strength of the samples was evaluated in terms of gel duration (G-dur) at 37 °C, which was measured by a previously reported method.[23] Briefly, a pre-weighed test tube containing 1 mL of the sample was equilibrated at 37 °C; the weight of the remaining sample was calculated from the difference in the weight of the tube. PBS medium (2 mL) was equilibrated at 37 °C and carefully layered over the surface of the gel. Tubes containing the sample and PBS medium were placed in an incubation chamber (SI-900R, Jeio Tech, Daejeon, Korea) maintained at 37 °C. After predetermined time intervals, the entire volume of PBS medium was removed and the weight of the test tube was measured. The percentage of gel erosion was obtained from the weight difference and plotted as a function of time. G-Dur was calculated for a reduction of weight >90% by the extrapolation of the percentage of decreased weight versus the time plot. All measurements were performed in triplicate.

Drug release from liposomal gels

The in vitro drug release of R-CL/P407 and R-FL/P407 was investigated using a membrane-less diffusion method with test tubes as previously reported.[35] An aliquot (1 mL) of the sample was gently distributed into the pre-weighed test-tube and equilibrated to 37 °C by placing in a water bath until gel formation occurred. Then, 2 mL of the release medium (pH 7.4 PBS containing 0.5% sodium lauryl sulfate) pre-equilibrated at 37 °C was carefully layered over the surface of the liposomal gel and the tube was placed in an incubation chamber at 37 °C. At pre-determined time points, the whole medium was collected for HPLC analysis and replaced by the same amount of fresh medium. To confirm the release of liposomal vesicles, the collected media were subjected for the preliminary observation of particle size distribution and ZP measurement as described above. The cumulative amount of released Rap (%) was calculated according to the following equation:

$$\text{Released Rap } (\%) = \left(\frac{\mathrm{V} \sum_{1}^{n-1} C_i + \mathrm{V}\, C_n}{m_o} \right) \times 100$$

where V is the volume of release medium (2 mL), C_i and C_n are the drug concentrations at the sampling timepoints, and m_o is the total amount of drug in the gel. Separation of free Rap from liposomal Rap was carried out by ultracentrifugation (14,000 g, 15 mins) using Amicon® ultracentrifugal filters (MWCO 100 kDa). Rap-encapsulating liposomal pellets were lysed using Triton X-100 (0.5% w/v). The filtrate and the lysed sample were each subjected to HPLC analysis as above. Simultaneously, according to the gravimetric method,[23] gel erosion (%) was evaluated by determining the weight changes after emptying the release medium and calculated using the following equation: $[(W_0–W_t)/W_0] \times 100$ (%), where W_0 and W_t are the initial weight of liposomal gel loaded into a tube and the final weight of liposomal gel remaining in the tube at time t, respectively.

In vivo antitumor efficacy in an orthotopic bladder cancer mouse model

Prior to the efficacy evaluation, an orthotopic bladder cancer mouse model was established as previously reported.[36] Briefly, female C3H mice at 5 weeks of age (Orient Bio Co., Seongnam, Korea) were purchased and held for an acclimation period of 1 week. MBT2 cells expressing luciferase (MBT2/Luc; 2.0×10^6 cells in PBS) were then instilled via the urethra using a 24-gauge catheter (i.d. 0.31 mm; o.d. 0.55 mm; length 19 mm). After six days, D-luciferin, a substrate for luciferase, was administered at 150 mg/kg by intraperitoneal injection, and bioluminescence was detected using an in vitro imaging system (IVIS) (Lumina XRMS Series; PerkinElmer Inc., Waltham, MA, USA) to evaluate tumor growth. The animal experiment was approved by the Institutional Animal Care and Use Committee of Chung-Ang University (2019–00061, Seoul, Korea), National Cancer Center Research Institute (NCC-15-257B, National Cancer Center, Goyang, Korea) and was carried out in accordance with the National Institute of Health Guidelines for the Care and Use of Laboratory Animals.

To evaluate in vivo antitumor efficacy, a total of 21 mice were randomly divided into three groups (n=7 for each group): group 1 received P407 hydrogel (Control); group 2 received R-CL/P407; and group 3 received the R-FL/P407. The instilled Rap dose was 1 mg/kg. The prepared formulations (50 μL) were instilled into the bladder lumen via urinary catheterization and each treatment was retained in the bladder for 2 hrs by tying off the orifice of

the urethra. The mouse was observed for cancer progression using an IVIS every 3–4 days and the instillation was performed one day after IVIS imaging to avoid extreme stresses. The bioluminescence signal (BLS) was acquired and analyzed using Living Image software version 2.50 (Xenogen, Alameda, CA, USA). Regions of interest (ROI) from displayed images were drawn manually around the BLS and quantified.[36] On day 14, all mice were sacrificed by CO_2 asphyxiation and the bladders were harvested. The harvested bladders were frozen in liquid nitrogen and then homogenized in protein extraction buffer for Western blot analysis.

Statistical analysis

Values are presented as the means ± standard deviation (n≥3). Statistical significance was determined using the Student's *t*-test and considered significant at $P<0.05$, unless otherwise stated.

Results and discussion

Characteristics of prepared liposomes

Liposomal systems composed of SPC and cholesterol were prepared and further surface-modified with folate by introducing $DP_{2K}F$. The addition of $DP_{2K}F$ was first optimized via a cell uptake study using DiI as a fluorescent probe. In all cell lines tested, MFI gradually increased with increasing $DP_{2K}F$ addition up to 0.5 mol% but did not increase beyond this level (Figure 2A). Thus, $DP_{2K}F$ addition was fixed at 0.5 mol% throughout the subsequent experiments. The physical characteristics of the prepared liposomes in either the empty (CL and FL) or Rap-loaded (R-CL and R-FL) state were evaluated in terms of particle size, size distribution, EE, and DL (Table 1). The average size of prepared liposomes ranged from 150–160 nm with a PDI value <0.2, indicating a homogenous dispersion. Neither Rap encapsulation nor surface modification with folate altered the liposomal size although the latter increased the ZP approximately 2-fold, which might be due to the presence of negatively charged functional groups derived from the $DP_{2K}F$ anchored on the liposomal bilayer. This result was in accordance with an earlier report that folate-modification imparted negative charge on the surface of the liposomes.[20] Both types of Rap-loaded liposomes (R-CL and R-FL) exhibited relatively low EE and DL, which might be attributed to the hydrophobicity of Rap, which was mainly localized into the

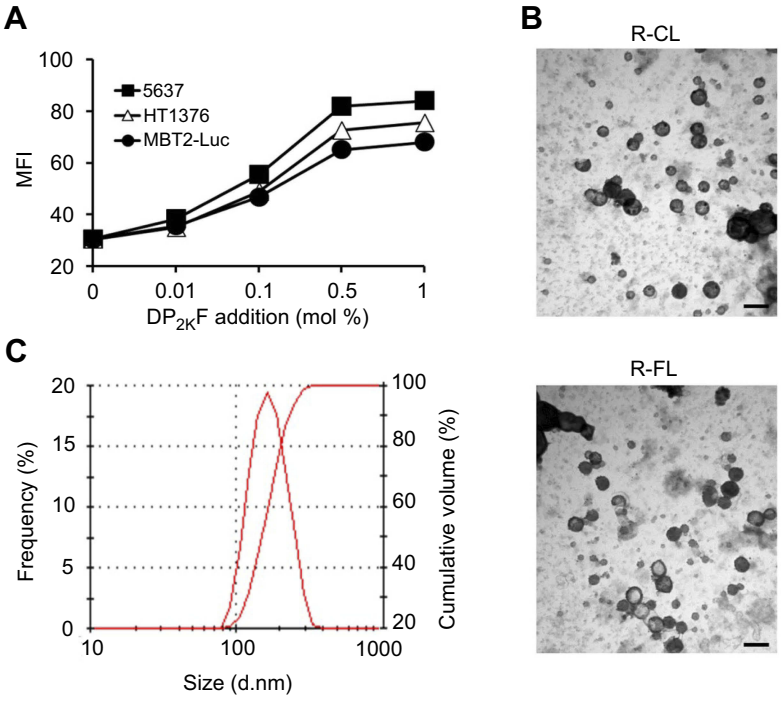

Figure 2 Characterization of prepared liposomes.

Notes: (**A**) Optimization of ligand density of R-FL evaluated by flow cytometry. Liposomes were loaded with DiI for MFI quantification. (**B**) Transmission electron microscopy images of liposomes. Scale bar indicates 200 nm. (**C**) Size distribution of R-FL by frequency. Data represent the means ± SD (n=3).

Abbreviations: MFI, mean fluorescence intensity; $DP_{2K}F$, distearoylphosphatidylethanolamine-polyethylene $glycol_{2000}$-folate; R, rapamycin; R-CL, rapamycin-loaded conventional liposome; R-FL, rapamycin-loaded folate-modified liposome.

Table 1 Composition and physical characteristics of prepared liposomes

	Empty liposomes		Rap-loaded liposomes	
	CL	**FL**	**R-CL**	**R-FL**
Composition (mol ratio)				
SPC	90	89.5	90	89.5
Cholesterol	10	10	10	10
$DP_{2K}F$	–	0.5	–	0.5
Rap (added)	–	–	10	10
Physical properties				
Size (nm)	155.8±0.21	157.1±0.77	156.7±0.84	158.8±0.24
PDI	0.18±0.02	0.17±0.04	0.14±0.02	0.18±0.03
ZP (mV)	−7.59±0.62	−16.49±0.61	−8.01±0.27	−17.26±0.25
EE (%)	–	–	42.4±0.47	42.1±0.22
DL (μg/mg)	–	–	57.32±0.41	56.67±0.29

Notes: Values represent the mean ± SD (n=3).
Abbreviations: CL, conventional liposome; FL, folate-modified liposome; R-CL, rapamycin-loaded conventional liposome; R-FL, rapamycin-loaded folate-modified liposome; SPC, soy phosphatidylcholine; $DP_{2K}F$, distearoylphosphatidylethanolamine-polyethylene $glycol_{2000}$-folate; Rap, rapamycin; PDI, polydispersity index; ZP, zeta potential; EE, entrapment efficiency; DL, drug loading.

phospholipid bilayer.[26] In addition, folate-modification did not alter the degree of Rap encapsulation in the liposomes, as evinced by negligible difference between R-CL and R-FL. In addition, similar results were obtained when the fluorescent probe DiI was introduced instead of Rap in the same liposomal preparations (Table S1).

R-CL and R-FL both presented spherical shape, which did not differ significantly (Figure 2B). The size distribution of both systems was narrow and unimodal, mostly in the range of 100–300 nm. A representative size-frequency curve of R-FL is depicted in Figure 2C. Based on these properties, both nanocarrier systems might be beneficial for drug delivery to tumoral tissues as nanocarriers with particle size <500 nm can readily pass across the enlarged gap junctions, leading to well-recognized enhanced permeation and retention effects.[37,38] In addition, it has been reported that spherical particles are normally readily taken up by cancer cells owing to the shorter membrane wrapping time for internalization.[39] Furthermore, the folate-modification on the surface may render R-FL as desirable for cancer-specific delivery.

Colloidal dispersion stability of prepared liposomes

The colloidal stability of R-FL was evaluated during storage at 4 °C and 25 °C for 4 weeks. As shown in Figure 3, R-FL was stable at 4 °C in terms of particle size, PDI, ZP, and drug loading, which were consistently maintained throughout the experiment. Similar behaviors were obtained with R-CL (Figure S1), indicating that both liposomes had excellent colloidal stability. The presence of cholesterol in the liposomal bilayer may contribute to the stability enhancement by increasing the packing of phospholipid molecules and improving vesicle resistance to aggregation.[40] For example, the in vitro and in vivo stability of liposomes composed of egg phosphatidylcholine and cholesterol was dependent on the cholesterol content, suggesting that liposomes containing 10% molar ratio of cholesterol are stable for up to 10 weeks at 4 °C.[41] In addition, the presence of cholesterol may have contributed to the rigidity of the liposomal bilayer thus rendering the membrane less permeable, which might underlie the negligible changes in the drug loading amount after 1 month at 4 °C.[42] Specifically, the high ZP-values in R-FL might be helpful for stabilizing the colloidal dispersion through the repulsive force between the particles.[43]

In comparison, during storage at 25 °C, slight changes were observed, revealing significant difference at $P<0.05$ for several time points. In particular, an increasing trend in particle size was observed and size distributions broadened, as evidenced by PDI values >0.3 after 4 weeks, even though no visual aggregation was observed. In turn, ZP-values were slightly decreased, although the values were still high enough to ensure sufficient repulsion to inhibit particle aggregation. Drug loading was also slightly decreased, indicating that drug leakage may have accelerated as the temperature increased. Numerous studies have reported that with increasing

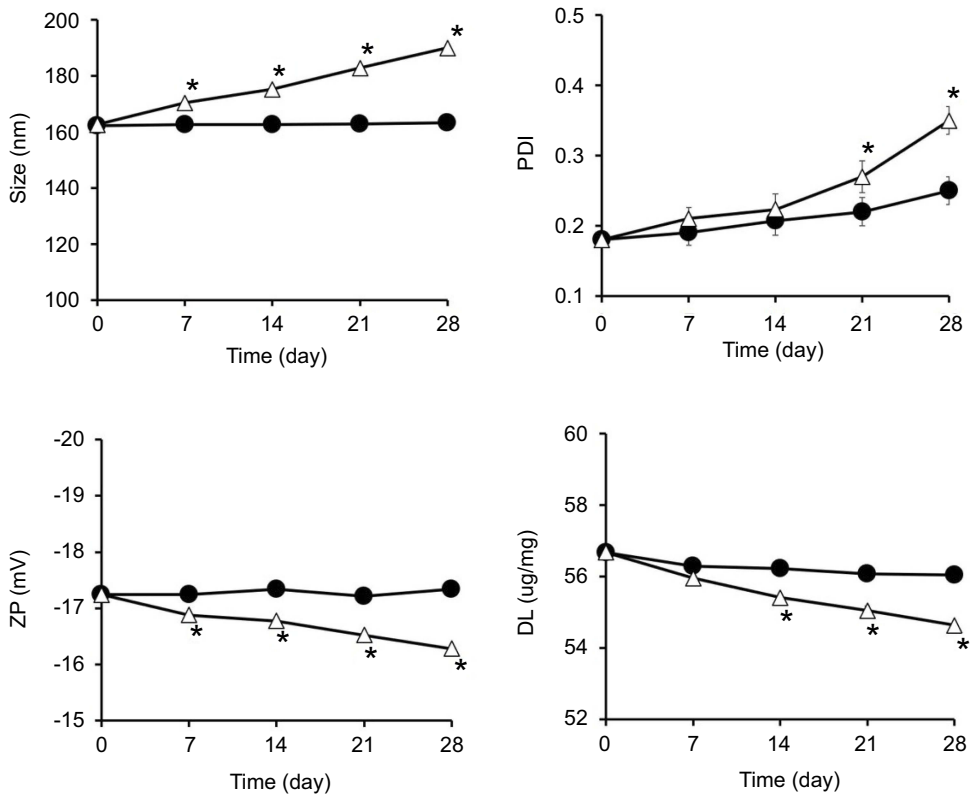

Figure 3 Stability evaluation of R-FL during storage at 4 °C (●) and 25 °C (△) for 4 weeks.
Notes: Statistical analysis was performed using the Student's *t*-test (*P<0.05 versus 4 °C). Data represent the means ± SD (n=3).

temperature, randomization in the hydrocarbon chain packing of the bilayer occurs, thereby reducing the membrane rigidity.[44] Thus, considering the instability of liposomes at elevated temperatures, the prepared liposomes were stored at 4 °C throughout the study and used for subsequent experiments within 7 days.

Cellular uptake behavior of the liposomes

To visualize the cell uptake behavior, DiI was used as a hydrophobic fluorescent probe, yielding a stable vesicle in terms of particle size and no significant leakage for at least 72 hrs in all liposomal preparations. Prior to the cellular uptake evaluation, the expression of FR protein was verified by Western blotting in the selected cell lines (5637, HT1376, and MBT2), which fell into the high positive category for FR expression. As shown in Figure 4A, all cell lines expressed FR-α at substantial levels, even though the level of expression differed, revealing the order of 5637> HT1376 ≫ MBT2. Using these FR+ cell lines, to confirm the folate selectivity of FL, quantification of the cellular uptake of liposomes was evaluated using flow cytometry (Figure 4B). In all cell lines, the fluorescence curves were shifted to the right by the liposomal formulation-treatment compared with those of untreated cells (Isotype). The degree shift from FL was greater than that from CL, indicating that folate modification markedly enhanced the cellular uptake. The internalization of FL into MBT2 cells was less than that into other cells, which might be due to the relatively lower level of FR expression in MBT2 cells among the studied cell lines as folate-mediated biomolecule uptake is well-recognized to be proportional to the FR density on the membrane of target cells.[45] To address this issue, in a previous study we designed multifunctional liposomal nanocarriers for FR-specific intracellular drug delivery using folate and Pep-1 peptide as a dual ligand for surface modification.[20]

Furthermore, to confirm the FR-mediated intracellular uptake of FL, a competitive assay was performed via challenge with folic acid. As shown in Figure 4C, in all cell lines, the cellular uptake level of FL was significantly suppressed by folic acid-pretreatment. MFI values in the folic acid-untreated group differed according to cell type, resulting in decreasing order of 5637 (84.2) > HT1376 (72.2) > MBT2 (60.1), whereas the values were similar (approximately 38.2) in all cell lines for the folic acid-pretreated group. These

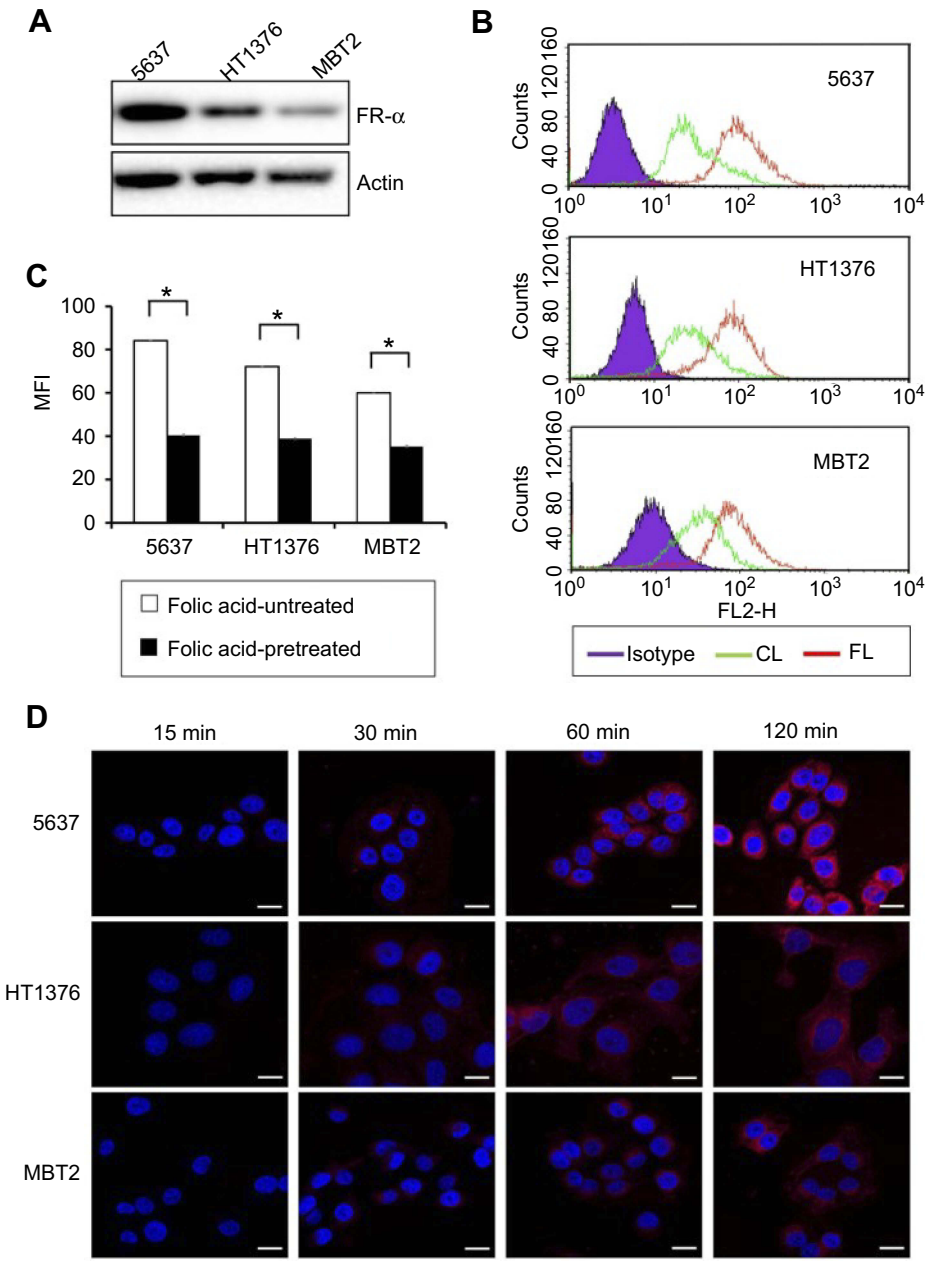

Figure 4 FR expression and comparison of the liposomal cell uptake in FR-positive cell lines.
Notes: (**A**) Western blot for FR-expression. GAPDH was used as a loading control to ensure the equal loading of gels. (**B**) Flow cytometry results for treatment effect after 2 h incubation. (**C**) Competitive assay of FL internalization under folic acid-untreated or folic acid-pretreated condition. (**D**) Confocal images for the time-dependent intracellular translocation of FL. White scale bar represents 100 μm. Data represent the means ± SD (n=3). Statistical analysis was performed using the Student's *t*-test (*$P<0.05$ versus the paired group).
Abbreviations: FR-α, folate receptor α; CL, conventional liposome; FL, folate-modified liposome.

findings indicated that free folic acid competed with folate-conjugates and inhibited the FR-mediated internalization, wherein the degree of competition was dependent on the level of FR expression. In addition, we also investigated the time-dependent translocation behavior of FL using CLSM (Figure 4D). During the initial 15 mins, no fluorescence was observed regardless of cell type. Subsequently, intracellular translocation was time- and cell type-dependent. After 30 mins, compared with the negligible fluorescence in MBT2 cell lines, weak red-fluorescence appeared on the cell surface of 5637 and HT1376 cell lines, the intensity of which gradually increased over time. After 2 hrs, scattered dot-like fluorescence appeared throughout the cytoplasm of HT1376 and MBT2 cell lines, whereas strong fluorescence

appeared in 5637 cells. These results are consistent with numerous reports highlighting the efficiency of FR-specific drug targeting.[46,47]

Enhanced growth inhibitory effects of Rap-loaded formulations in URCa cell lines

Next, we evaluated whether R-FL could enhance the growth inhibition in URCa cell lines expressing FR. Treatment with Rap, R-CL, or R-FL yielded cytotoxicity effects in URCa cell lines in a dose-dependent manner between 24 and 72 hrs of exposure time (Figure 5A). Exposure of the 5637 cell line to Rap or to R-CL at low concentration (1 μg) for 48 hrs resulted in only <10% decreased cell viability; however, treatment with R-FL reduced viability by 40%. HT1376 cells exhibited the greatest sensitivity to all Rap-formulations among the tested URCa cell lines, with 10 μg R-FL treatment for

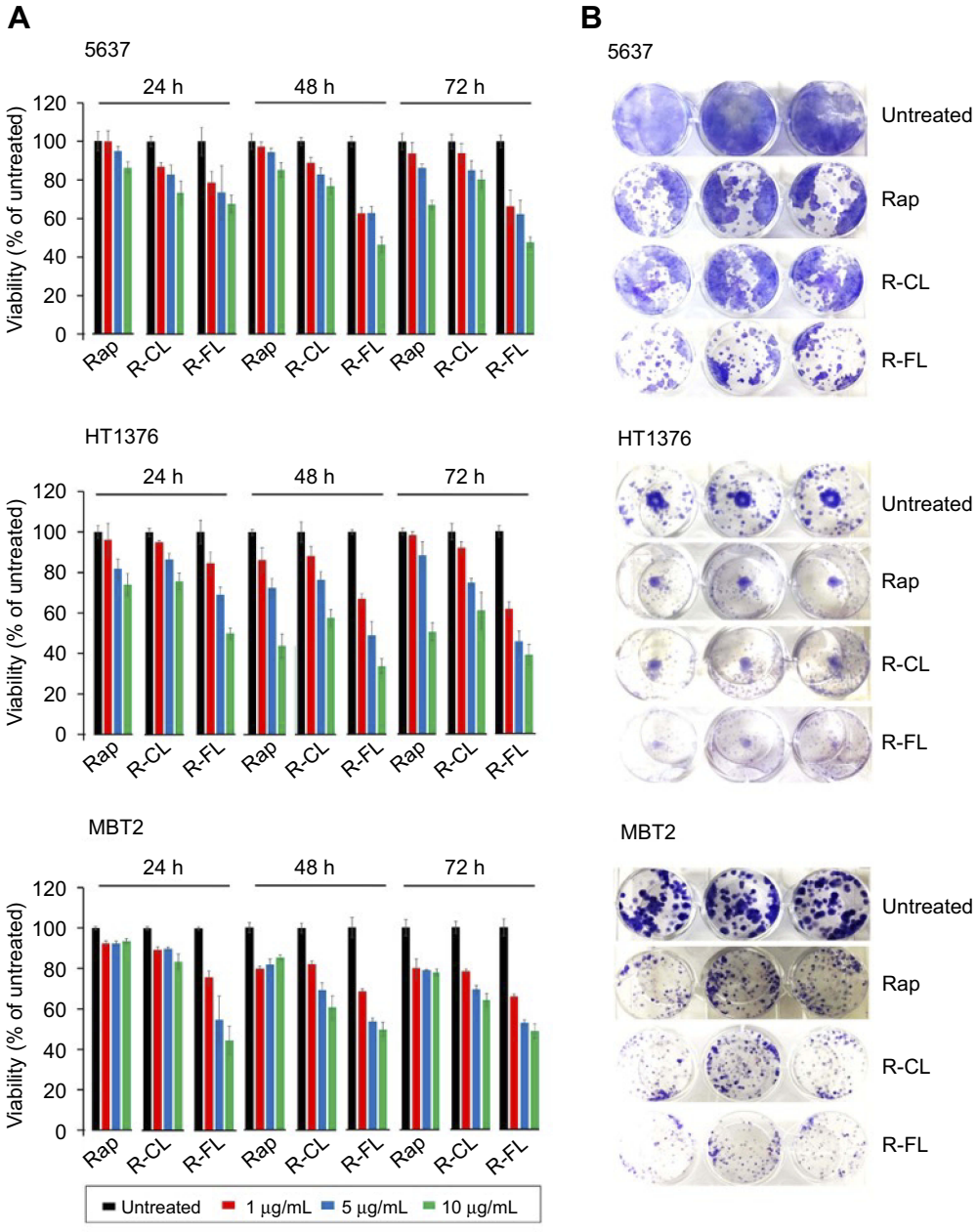

Figure 5 Effects of Rap-loaded formulations on growth inhibition in URCa cells.

Notes: (**A**) MTT assay with various concentration of Rap-loaded formulations. Data represent the means ± SEM (n=6). (**B**) Colony forming assay with Rap-loaded formulations (1 μg/mL).

Abbreviations: Rap, rapamycin; R-CL, rapamycin-loaded conventional liposome; R-FL, rapamycin-loaded folate-modified liposome.

24 hrs inducing <50% decrease of cell viability compared to that from Rap or R-CL. Notably, even the low FR-expressing MBT2 cell line exhibited 50% reduction in cell viability upon exposure to 10 μg R-FL for 24 hrs. Thus, R-FL could induce cytotoxicity more effectively than Rap or R-CL depending on the cell type and experimental conditions. Similarly, treatment with R-FL at a concentration of 1 μg resulted in the largest inhibitory effect on the anchorage-dependent colony forming activity of the 5637 cell line compared to that from Rap or R-CL (Figure 5B). Furthermore, R-FL induced >60% decrease in the anchorage-independent colony forming ability of the MBT2 cell line although it only slightly enhanced the inhibitory effect of Rap on this ability in the HT1376 cell line. Taken together, these results suggested that R-FL may have fortified the activities of Rap in suppressing the viability and tumorigenic potential of URCa cell lines.

mTOR inhibition and autophagy induction of Rap-loaded formulations in URCa cell lines

Rap, which functions as an mTOR inhibitor in mammalian cells, has been widely applied as an immunosuppressive and anticancer therapeutic agent through enhancing T-cell immunity[48] and suppressing tumor cell growth.[49] Rap-sensitive mTOR complex 1 (mTORC1) regulates translational signaling through phosphorylation of the p70 ribosomal protein S6 kinase (p70S6K) and eukaryotic initiation factor 4E binding protein 1 (4EBP-1).[50,51] Hypothesizing that mTOR phosphorylation at Ser2448 is blocked by Rap, we next evaluated the effect of Rap, R-CL, and R-FL on mTOR Ser2448 phosphorylation, which in turn targets p70S6K and 4EBP-1.[52] All Rap-loaded formulations inhibited mTOR signaling along with the downstream proteins (Figure 6A), which was not consistent with the finding that URCa cell lines exhibited the highest sensitivity to R-FL (Figure 5). Therefore, these results suggested that the R-FL-induced growth inhibition in URCa cells did not directly involve inhibition of the mTORC1 activity.

Next, we sought to determine the relative activation of adenosine monophosphate-activated serine/threonine protein kinase (AMPK) upon treatment with Rap-loaded formulations, along with that on the beneficial AMPK–mTORC1 signaling pathway, which serves as a target for cancer treatment.[53,54] As shown in Figure 6B, R-FL treatment induced phosphorylation of AMPK in all URCa cell lines, even though Rap or R-CL yielded greater induction in the HT1376 cell line. Notably, it has been reported that mTOR and AMPK can induce phosphorylation of the autophagy-inducing protein ULK-1 at distinct sites.[55,56] Moreover, activated mTORC1 suppresses ULK1 by phosphorylating it at Ser 757, whereas downregulation of mTORC1 activity in turn led to phosphorylated ULK1 (Ser 555) by AMPK activation, resulting in subsequent autophagic initiation.[57] Therefore, we asked whether R-FL treatment could activate autophagy-initiation proteins consequent to the activation of AMPK in URCa cells. As expected, R-CL and R-FL suppressed ULK1 phosphorylation at Ser 555 and induced phosphorylation at Ser 757 in URCa cell lines. Consistent with the result from the activation of AMPK-mTORC1 signaling by R-CL or R-FL, ULK1 phosphorylation at Ser 555 was reduced to a greater extent in the R-CL- or R-FL-treated cell lines compared to that in Rap-treated cells. This effect was sufficient to induce autophagy initiation by suppression of ULK1 phosphorylation at Ser 555 even when Rap treatment could not induce AMPK activation in the MBT2 cell line, potentially through release from the mTORC1-suppressed ULK1 phosphorylation at Ser 757.

Furthermore, to confirm that the R-FL-induced autophagy initiation was related to auotophagosomal elongation for the induction of cell death, Beclin, p62, ATG5, and LC3-I/II in URCa cell lines were assessed upon treatment with Rap or R-FL (Figure 6C). Bafilomycin A1 (Baf), an inhibitor autophagic vacuole maturation, was used as a positive control. No significant changes in autophagosomal elongation-related proteins were observed in URCa cell lines treated with Rap or R-FL. However, Baf induced an accumulation of p62 and ATG5 in all URCa cell lines, whereas Beclin-1 was slightly induced in Baf-treated HT1376 and MBT2. The increases in LC3-II accumulation were observed in URCa cell lines treated with Baf, resulting in blockage of the autophagosomal elongation to complete autophagy. Therefore, treatment with Rap or R-FL led to switching from autophagy to the synergistic induction of cell death. Moreover, it has been reported that Rap is the most potent inducer of autophagy,[58] which is consistent with the result shown in Figure 6B and C, indicating a similar role as Rap-induced autophagy. Because p62 and ATG5 accumulate and aggregate when autophagy is inhibited,[59] inhibition of this behavior might result from Baf treatment in the URCa cell lines. Furthermore, we observed increases in LC3-II accumulation in URCa cell lines treated with Baf, resulting in blockage of the autophagosomal elongation to complete autophagy. Consistent

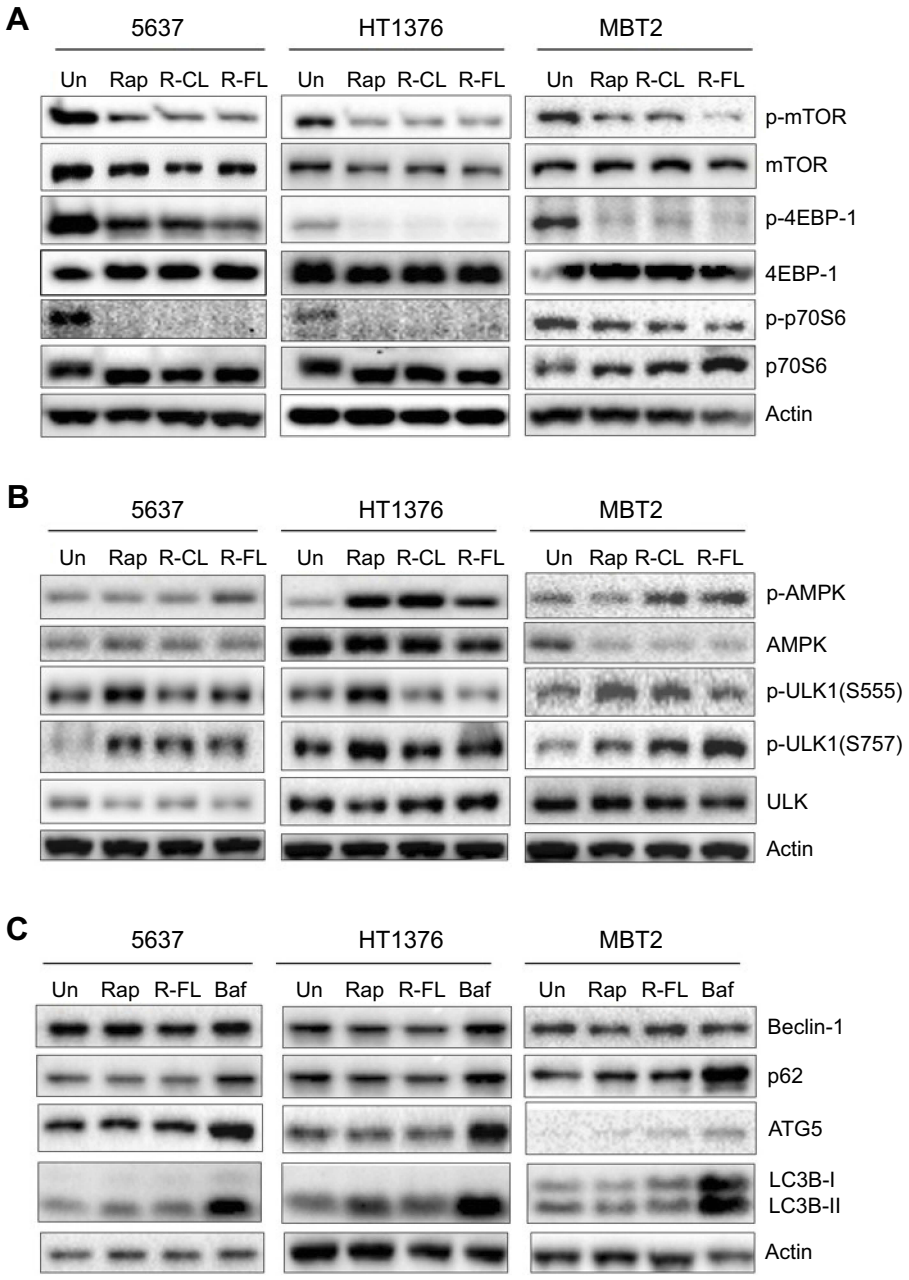

Figure 6 Effects of Rap-loaded formulations on mTOR inhibition and autophagy induction in URCa cells.
Notes: (**A**) Inhibition of phosphorylation of mTOR and mTOR downstream proteins. (**B**) Induction of AMPKα activation and ULK phosphorylation at Ser757. (**C**) Accumulation of p62/ATG5 and cleaved LC3B-II. Actin was used as a loading control.
Abbreviations: Un, untreated; Rap, rapamycin; R-CL, rapamycin-loaded conventional liposome; R-FL, rapamycin-loaded folate-modified liposome; Baf, bafilomycin A1.

with this, a recent study demonstrated that autophagy may function as a potential antitumor mechanism; in addition, Rap exhibits anticancer activity against human tumors by inducing autophagy.[60] Therefore, our findings suggested that the inhibition of mTOR phosphorylation and induction of autophagy through the activation of AMPK in Rap-loaded liposomes could enhance the sensitivity to Rap in URCa cell lines.

Characteristics of gel formulations

The thermo-sensitive gel-forming capacities of the drug/liposome-free P407 hydrogel (P407-Gel) and Rap-loaded liposome-dispersed P407-Gel (R-CL/P407 and R-FL/P407) were evaluated with regard to G-Temp, G-Time, and G-Dur (Table 2). P407-Gel exhibited similar results as in an earlier report:[23] G-Temp 21 °C; G-Time 29.1 seconds; and G-Dur 12.13 hrs. Liposomal dispersion did not affect the gel-

Table 2 Gel forming capacities of Rap-free P407 and Rap-loaded liposomal gel

	P407-Gel	R-CL/P407	R-FL/P407
G-Temp (°C)	21	21	21
G-Time (seconds)	29.1±0.3	28.9±0.5	28.7±0.7
G-Dur (hours)	12.13±0.3	12.09±0.1	12.11±0.1

Note: Values represent the mean ± SD (n=3).
Abbreviations: G-temp, gelation temperature; G-time, gelation time; G-Dur, gel duration; Rap, rapamycin; P407-Gel, poloxamer 407-based hydrogel; R-CL/P407, rapamycin-loaded conventional liposome dispersed in P407-Gel; R-FL/P407, rapamycin-loaded folate-modified liposome dispersed in P407-Gel.

forming property, indicating that no interactions occurred between liposomes and P407. The G-Temp below room temperature was expected to indicate gelation following intravesical instillation, whereas the gel exists in a fluid-state under refrigerated storage. The G-Time within 30 seconds was considered appropriate to effect rapid gelation in the bladder to avoid dilution by urine. These values indicated that the prepared formulations exist in liquid-state but would transform into gel shortly following instillation into the bladder. The G-Dur over 12 hrs might be sufficient to support therapeutic effect as the urination-restricted period in conventional intravesical therapy is generally a 2 hr-cycle.[61] Thus, we expect that the liposomal gels would not completely be eliminated by a single urination but undergo partial erosion, liberating the liposomal vesicles and thereby providing a better environment for Rap therapy. Owing to these thermoreversible gelation properties, it is expected that the liposomal gel formulation would contribute to increased contact time in the bladder, of which the temperature is around 37 °C.

In vitro drug release from liposomal gels

Drug release profiles of liposomal gels were evaluated by measuring the amount of liposomal Rap and free Rap separately. As shown in Figure 7A, the cumulative amount of liposomal Rap (R-CL and R-FL) increased linearly (R^2>0.99) with time, indicating zero-order release kinetics. However, the release of free Rap was negligible, representing <5% over 12 h. Thus, it appeared that Rap release took place while encapsulated in the liposomal vesicles, without molecular diffusion of the free drug. In this case, the liposome may act as a reservoir within the gel matrix, lowering the

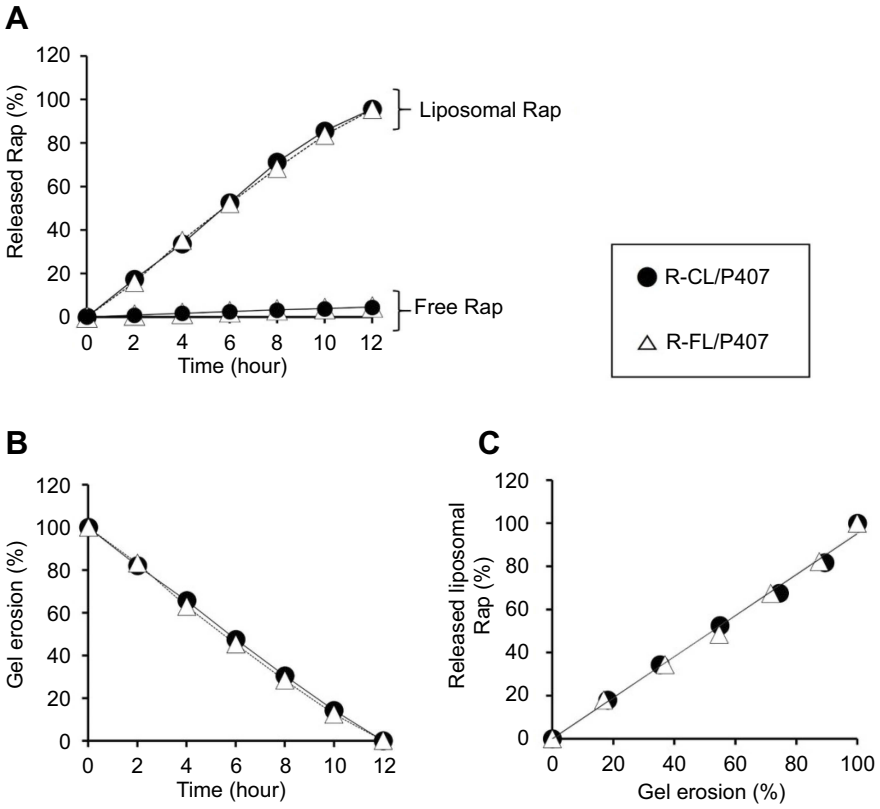

Figure 7 Drug release and gel erosion characteristics of Rap-loaded liposomal gels.
Notes: (**A**) In vitro drug release profile as a function of time. (**B**) Gel erosion profile as a function of time. (**C**) Correlation between liposomal Rap release and gel erosion. Data represent the means ± SD (n=3).
Abbreviations: Rap, rapamycin.

diffusion rate from the inner gel structure to the outer medium.[32] The release of liposomal vesicles was further verified by observing the size distribution of any particulates in drug release medium, of which the size and ZP of R-CL/P407 and R-FL/P407 samples were determined as 158.5 nm and 160.1 nm on average, and −7.56 mV and −15.19 mV, respectively, in three independent experiments. These results were nearly close to the size and ZP of Rap-loaded liposomes, indicating that liposomal vesicles released intact from the gel matrix while encapsulating Rap. Moreover, during the release study, we found that the mass of gel matrix gradually decreased over time. Figure 7B depicts the gel erosion behavior by plotting the weight of the remaining gel against the time. The graphs revealed a linear decrease, suggesting zero-order decay in both R-CL/P407 and R-FL/P407.

To further interpret the drug release behavior of both liposomal gels, the relationship between the gel erosion and the Rap release was analyzed (Figure 7C). Good linearity with a high correlation coefficient (R^2>0.99) was observed, indicating that Rap was released from the gels in an erosion-controlled manner. Considering the experimental set-up using the membrane-less method, in which the gel is not confined by a membrane but rather placed in an aqueous environment, gel erosion might reasonably represent a predominant factor.[62] In addition, drug diffusion from the gel mainly depends on the mesh size within the gel matrix, with the hydrodynamic radius of the drug molecule playing a concordantly important role.[63] A typical mesh size of the hydrogel in its swollen state was reported as 5–100 nm,[64] whereas the size of R-CL and R-FL was approximately 150–160 nm, implying that rather than molecular diffusion, gel erosion served as a main driving mechanism for Rap release from liposomal gels. Therefore, we could expect that, after intravesical administration of liposomal gel, Rap-encapsulating liposomes would be released first into the bulk medium by means of gel erosion, followed by intimate contact of the liposomal vesicles with biological membranes for permeation. This behavior might be beneficial for successful intravesical drug delivery by providing prolonged drug delivery, ensuring efficient drug exposure to tumor tissues.

In vivo antitumor efficacy of liposomal gels in an orthotopic bladder cancer mouse model

To evaluate the antitumor activity of liposomal gel formulations in vivo, we successfully established an orthotopic bladder cancer model using C3H mice by intravesical instillation of MBT2/Luc cells. Six days after tumor implantation, all mice produced BLS and thus were randomly divided into three treatment groups (designated as day 0). There was no significant difference in BLS intensity between groups at the time of randomization. BLS from the ROI was expressed using a colored scale, with red representing the most intense BLS and blue representing the least intense BLS (Figure 8A). From day 4, the scale was normalized to eliminate any possible disturbance from the background signal and to facilitate the relative comparison of tumor growth between treatment groups. In the control group, the red-colored BLS increased with time, indicating the tumor growth. However, in Rap-loaded liposomal gel-treatment groups, the red signals became weaker and/or even absent, representing the effective suppression of tumor growth. Specifically, R-FL/P407 was most effective, showing no or weak red-signals with significantly reduced progression. To compare the tumor growth quantitatively, the changes in BLS were expressed as ROI (Figure 8B).[33] For the first 4 days, the control group showed a slight increase in ROI values, whereas R-CL/P407- and R-FL/P407-treated groups revealed little or negligible changes. Similar trends were observed at 7 days; however, significant differences were observed between treatment groups after this period, including steep increase in the control group, moderate increase in the R-CL/P407 group, and mild increase in the R-FL/P407 group. The R-CL/P407 and R-FL/P407 groups differed significantly on day 11 (P=0.0273) and day 14 (P=0.0088). Thus, owing to FR-target functionality, R-FL/P407 was superior to R-CL/P407 in suppressing tumor growth.

At the termination of the experiment, Western blotting was performed on harvested tumors to evaluate the efficacy of Rap (Figure 8C). The tumors from the mice treated with R-FL/P407 revealed reduction of the levels of mTOR phosphorylation, which induced downregulated phosphorylation of p70S6 and 4EBP-1 as compared with the levels in control and R-CL/P407-treated tumors. Moreover, R-FL/P407-treated tumors exhibited greater cleavage of the 113 kDa PARP molecule than that detected in the control or R-CL/P407-treated tumor. Consistent with the in vitro results, R-FL/P407 treatment downregulated the mTOR singling pathway and increased PARP cleavage (an apoptotic marker) in the orthotopic bladder cancer mouse model. These results suggested that R-FL/P407 significantly retards tumor growth in vivo by inducing apoptosis through inhibition of mTOR phosphorylation

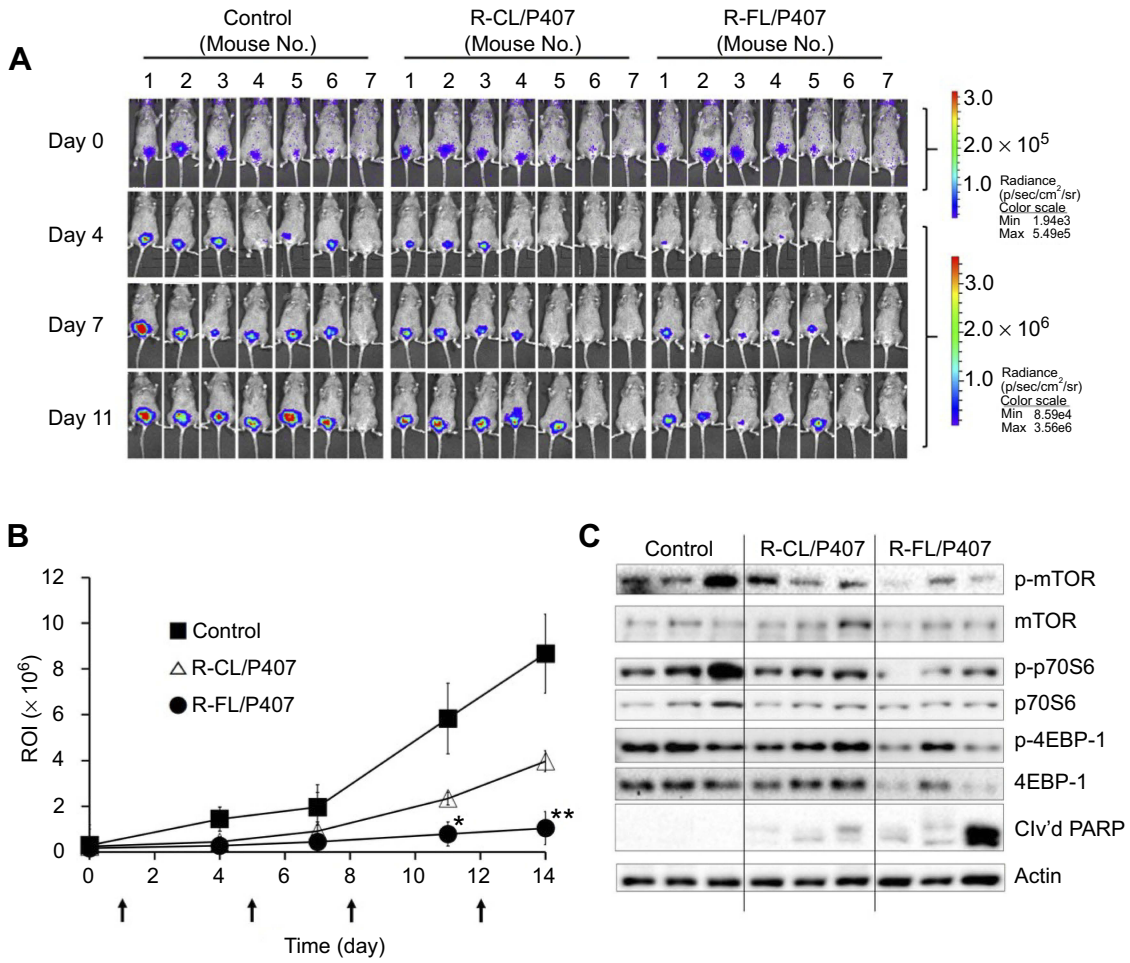

Figure 8 Comparison of in vivo antitumor efficacy of different samples in the orthotopic bladder cancer model in C3H mice.

Notes: (**A**) In vivo imaging acquired via BLS. For statistical analyses, tumor bioluminescence following treatment was normalized against the initial bioluminescence on day 4. (**B**) ROI-time plots for quantitative comparison (*P<0.05, **P<0.01 versus R-CL/P407). Arrows indicate instillations. Data represent the means ± SD (n=7). (**C**) Inhibition of mTOR signaling and induction of cleaved PARP. The blots are representative of three independent experiments.

Abbreviations: R, rapamycin; R-CL, rapamycin-loaded conventional liposome; R-FL, rapamycin loaded folate-modified liposome; P407, poloxamer 407; BLS, bioluminescence signal; ROI, region of interest.

Significant suppression of tumor growth in the R-FL/P407-treated group might have occurred for several reasons. First, owing to the thermo-sensitive property of P407, liposomal gels formed in the bladder shortly after intravesical instillation of R-FL/P407, thus increasing the residence time that afforded a better environment for drug absorption. In general, intravesically administered drugs are easily washed-out or diluted by urination, highlighting the need for repeated administration.[13] In the present experiment, the liposomal gel was sufficiently durable (over 12 hrs of G-Dur), providing the potential to play a role as a drug reservoir. Second, continuous release of Rap-loaded liposomal vesicles from the hydrogel matrix would be beneficial for tumor suppression. As the main driving mechanism of Rap release from the gel matrix was regulated by erosion, the exposure of R-FL to bladder URCa cells could be extended for a longer period. Third, the FR-mediated endocytosis might further facilitate the drug absorption. Folate-modified liposomal nanocarriers would efficiently bind to FR-expressing cancer cells, then intracellularly translocate by receptor-mediated endocytosis and liberate Rap to induce autophagy-mediated apoptosis. Overall, our findings indicate that extended residence time and continuous release of liposomal drugs in the bladder were realized by employing thermo-sensitive P407 hydrogels; ultimately, by virtue of the folic acid-modification, enhanced uptake of Rap was attained through increased adherence of liposomal vesicles to the bladder cancer cells. In the current study, rodents were used, but for a more reliable research basis, larger animals should be adopted regarding genetics and morphology to mimic the human bladder pathology and biochemical characteristics.

Conclusion

Rap-loaded folate-modified liposomal hydrogel (R-FL/P407) was successfully fabricated by encapsulating Rap into FL with homogeneous dispersion throughout the P407-based thermo-reversible hydrogels. Using FR-positive URCa cell lines, beneficial effects of R-FL were demonstrated with regards to cell growth inhibition, mTOR inhibition, and autophagy induction. Liposomal gel formulations exhibited good gelation properties and drug release from the gel matrix was erosion controlled. In the MBT2/Luc orthotopic bladder cancer mouse model, R-FL/P407-treated groups showed enhanced in vivo antitumor efficacy. Together, these findings indicate that R-FL/P407 might serve as a promising system for targeted Rap delivery to FR-expressing bladder cancer.

Abbreviations

AMPK, adenosine monophosphate-activated serine/threonine protein kinase; Baf, bafilomycin A1; BLS, bioluminescence signal; CLSM, confocal laser scanning microscopy; Dil, 1,1′-dioctadecyl-3,3,3′,3′-tetramethylindocarbocyanine perchlorate; DL, drug loading; $DP_{2K}F$, distearoylphosphatidylethanolamine-polyethylene glycol-$_{2000}$-folate; EE, entrapment efficiency; FR, folate receptor; G-dur, gel duration; G-temp, gelation temperature; G-time, gelation time; HPLC, high performance liquid chromatography; IVIS, in vitro imaging system; MFI, mean fluorescence intensity; mTORC1, mTOR complex 1; P407, poloxamer 407; PBS, phosphate buffered saline; PDI, polydispersity index; Rap, rapamycin; R-CL, Rap-loaded conventional liposomes; R-FL, Rap-loaded folate-modified liposomes; ROI, regions of interest; SDS-PAGE, sodium dodecyl sulfate-polyacrylamide gel electrophoresis; SPC, Soy phosphatidylcholine; URCa, urothelial carcinoma; ZP, zeta potential.

Acknowledgments

This research was supported by the Korea Health Industry Development Institute (KHIDI) funded by the Ministry of Health and Welfare, Republic of Korea (HI17C0710). This work was also supported by the National Research Foundation of Korea (NRF) grant funded by the Korea government (MSIT) (No. 2019R1A2C2002510).

Disclosure

The authors report no conflicts of interest in this work.

References

1. Shariat SF, Sfakianos JP, Droller MJ, Karakiewicz PI, Meryn S, Bochner BH. The effect of age and gender on bladder cancer: a critical review of the literature. *BJU Int*. 2010;105:300–308. doi:10.1111/j.1464-410X.2009.09076.x
2. Jensen TK, Holt P, Gerke O, et al. Preoperative lymph-node staging of invasive urothelial bladder cancer with 18F-fluorodeoxyglucose positron emission tomography/computed axial tomography and magnetic resonance imaging: correlation with histopathology. *Scand J Urol Nephrol*. 2011;45:122–128. doi:10.3109/00365599.2010.544672
3. Oliveira MB, Villa Nova M, Bruschi ML. A review of recent developments on micro/nanostructured pharmaceutical systems for intravesical therapy of the bladder cancer. *Pharm Dev Technol*. 2018;23:1–12. doi:10.1080/10837450.2017.1312441
4. Mattioli F, Curotto A, Manfredi V, et al. Intravesical gemcitabine in superficial bladder cancer: a phase II safety, efficacy and pharmacokinetic study. *Anticancer Res*. 2005;25:2493–2496.
5. Malmstro¨m. Intravesical therapy of superficial bladder cancer. *Crit Rev Oncol Hematol*. 2003;47:109–126. doi:10.1016/S1040-8428(03)00075-1
6. Packiam VT, Johnson SC, Steinberg GD. Non-muscle-invasive bladder cancer: intravesical treatments beyond Bacille Calmette-Guérin. *Cancer*. 2017;123:390–400. doi:10.1002/cncr.v123.3
7. Guduru SKR, Arya P. Synthesis and biological evaluation of rapamycin-derived, next generation small molecules. *Medchemcomm*. 2017;9:27–43. doi:10.1039/C7MD00474E
8. Wan X 1, Helman LJ. The biology behind mTOR inhibition in sarcoma. *Oncologist*. 2007;12:1007–1018. doi:10.1634/theoncologist.12-8-1007
9. Cloughesy TF, Yoshimoto K, Nghiemphu P, et al. Antitumor activity of rapamycin in a Phase I trial for patients with recurrent PTEN-deficient glioblastoma. *PLoS Med*. 2008;5:0139–0151. doi:10.1371/journal.pmed.0050008
10. Rouf MA, Vural I, Renoir JM, et al. Development and characterization of liposomal formulations for rapamycin delivery and investigation of their antiproliferative effect on MCF7 cells. *J Liposome Res*. 2009;19:322–331. doi:10.3109/08982100902963043
11. Seager CM, Puzio-Kuter AM, Patel T, et al. Intravesical delivery of rapamycin suppresses tumorigenesis in a mouse model of progressive bladder cancer. *Cancer Prev Res (Phila)*. 2009;2:1008–1014. doi:10.1158/1940-6207.CAPR-09-0169
12. Preetham AC, Satish CS. Formulation of a poorly water-soluble drug sirolimus in solid dispersions to improve dissolution. *J Dispers Sci Technol*. 2011;32:778–783. doi:10.1080/01932691.2010.488129
13. GuhaSarkar S, Banerjee R. Intravesical drug delivery: challenges, current status, opportunities and novel strategies. *J Control Release*. 2010;148:147–159. doi:10.1016/j.jconrel.2010.08.031
14. Horiguchi Y, Larchian WA, Kaplinsky R, Fair WR, Heston WD. Intravesical liposome-mediated interleukin-2 gene therapy in orthotopic murine bladder cancer model. *Gene Ther*. 2000;7:844–851. doi:10.1038/sj.gt.3301076
15. Vila-Caballer M, Codolo G, Munari F, et al. A pH-sensitive stearoyl-PEG-poly(methacryloyl sulfadimethoxine)-decorated liposome system for protein delivery: an application for bladder cancer treatment. *J Control Release*. 2016;238:31–42. doi:10.1016/j.jconrel.2016.07.024
16. Miyazaki J, Nishiyama H, Yano I, et al. The therapeutic effects of R8-liposome-BCG-CWS on BBN-induced rat urinary bladder carcinoma. *Anticancer Res*. 2011;31:2065–2071.
17. Kim CH, Lee SG, Kang MJ, Lee SK, Choi YW. Surface modification of lipid-based nanocarriers for cancer cell-specific drug targeting. *J Pharm Investig*. 2017;47:203–227. doi:10.1007/s40005-017-0329-5
18. Gupta B, Yong CS, Kim JO. Solid matrix-based lipid nanoplatforms as carriers for combinational therapeutics in cancer. *J Pharm Investig*. 2017;47:461–473. doi:10.1007/s40005-017-0337-5

19. Saul JM, Annapragada A, Natarajan JV, Bellamkonda RV. Controlled targeting of liposomal doxorubicin via the folate receptor in vitro. *J Control Release*. 2003;92:49–67.
20. Kang MH, Yoo HJ, Kwon YH, et al. Design of Multifunctional Liposomal Nanocarriers for Folate Receptor-Specific Intracellular Drug Delivery. *Mol Pharm*. 2015;12:4200–4213.
21. Kolawole OM, Lau WM, Mostafid H, Khutoryanskiy VV. Advances in intravesical drug delivery systems to treat bladder cancer. *Int J Pharm*. 2017;532:105–117. doi:10.1016/j.ijpharm.2017.08.120
22. Hadaschik BA. ter Borg MG, Jackson J, et al. Paclitaxel and cisplatin as intravesical agents against non-muscle-invasive bladder cancer. *BJU Int*. 2008;101:1347–1355. doi:10.1111/j.1464-410X.2008.07571.x
23. Kim SH, Kim SR, Yoon HY, et al. Poloxamer 407 Hydrogels for Intravesical Instillation to Mouse Bladder: gel-Forming Capacity and Retention Performance. *Korean J Urol Oncol*. 2017;15:178–186. doi:10.22465/kjuo.2017.15.3.178
24. Zhang L, Parsons DL, Navarre C, et al. Development and in-vitro evaluation of sustained release poloxamer 407 (P407) gel formulations of ceftiofur. *J Control Release*. 2002;85:73–81. doi:10.1016/S0168-3659(02)00273-0
25. Ju C, Sun J, Zi P, et al. Thermosensitive micelles-hydrogel hybrid system based on poloxamer 407 for localized delivery of paclitaxel. *J Pharm Sci*. 2013;102:2707–2717. doi:10.1002/jps.23649
26. Wickremasinghe NC, Kumar VA, Hartgerink JD. Two-step self-assembly of liposome-multidomain peptide nanofiber hydrogel for time-controlled release. *Biomacromolecules*. 2014;15:3587–3595. doi:10.1021/bm500856c
27. Majumder P, Baxa U, Walsh STR, Schneider JP. Design of a Multicompartment Hydrogel that Facilitates Time-Resolved Delivery of Combination Therapy and Synergized Killing of Glioblastoma. *Angew Chem*. 2018;130:15260–15264. doi:10.1002/ange.201806483
28. Li J, Mooney DJ. Designing hydrogels for controlled drug delivery. *Nat Rev Mater*. 2016;12:16071–16088. doi:10.1038/natrevmats.2016.71
29. Jang MH, Kim CH, Yoon HY, et al. Steric stabilization of RIPL peptide-conjugated liposomes and in vitro assessment. *J Pharm Investig*. 2019;49:115–125. doi:10.1007/s40005-018-0392-6
30. Sonali; Singh RP, Sharma G, et al. RGD-TPGS decorated theranostic liposomes for brain targeted delivery. *Colloids Surf B Biointerfaces*. 2016;147:129–141. doi:10.1016/j.colsurfb.2016.07.058
31. Wu W, He Z, Zhang Z, Yu X, Song Z, Li X. Intravitreal injection of rapamycin-loaded polymeric micelles for inhibition of ocular inflammation in rat model. *Int J Pharm*. 2016;513:238–246. doi:10.1016/j.ijpharm.2016.09.013
32. Whang YM, Park SI, Trenary IA. LKB1 deficiency enhances sensitivity to energetic stress induced by erlotinib treatment in non-small-cell lung cancer (NSCLC) cells. *Oncogene*. 2016;35:856–866. doi:10.1038/onc.2015.140
33. Whang YM, Kim YH, Kim JS, Yoo YD. RASSF1A suppresses the c-Jun-NH2-kinase pathway and inhibits cell cycle progression. *Cancer Res*. 2005;65:3682–3690. doi:10.1158/0008-5472.CAN-04-4557
34. Derakhshandeh K, Fashi M, Seifoleslami S. Thermosensitive pluronic hydrogel: prolonged injectable formulation for drug abuse. *Drug Des Devel Ther*. 2010;4:255–262. doi:10.2147/DDDT.S13289
35. Mao Y, Li X, Chen G, Wang S. Thermosensitive hydrogel system with paclitaxel liposomes used in localized drug delivery system for in situ treatment of tumor: better antitumor efficacy and lower toxicity. *J Pharm Sci*. 2016;105:194–204. doi:10.1002/jps.24693
36. Kim SY, Kwon WA, Shin SP. Electrostatic interaction of tumor-targeting adenoviruses with aminoclay acquires enhanced infectivity to tumor cells inside the bladder and has better cytotoxic activity. *Drug Deliv*. 2018;25:49–58. doi:10.1080/10717544.2018.1474967
37. Decuzzi P, Godin B, Tanaka T, et al. Size and shape effects in the biodistribution of intravascularly injected particles. *J Control Release*. 2010;141:320–327. doi:10.1016/j.jconrel.2009.09.007
38. Wicki A, Witzigmann D, Balasubramanian V, Huwyler J. Nanomedicine in cancer therapy: challenges, opportunities, and clinical applications. *J Control Release*. 2015;200:138–157. doi:10.1016/j.jconrel.2014.12.030
39. Verma A, Stellacci F. Effect of surface properties on nanoparticle-cell interactions. *Small*. 2010;6:12–21. doi:10.1002/smll.200901158
40. Kirby C, Clarke J, Gregoriadis G. Effect of the cholesterol content of small unilamellar liposomes on their stability in vivo and in vitro. *Biochem J*. 1980;186:591–598. doi:10.1042/bj1860591
41. Yang T, Cui FD, Choi MK, et al. Liposome formulation of paclitaxel with enhanced solubility and stability. *Drug Deliv*. 2007;14:301–308. doi:10.1080/10717540701606483
42. Briuglia ML, Rotella C, McFarlane A, Lamprou DA. Influence of cholesterol on liposome stability and on in vitro drug release. *Drug Deliv Transl Res*. 2015;5:231–242. doi:10.1007/s13346-015-0247-x
43. Vijayakumar MR, Kosuru R, Vuddanda PR, Singh SK, Singh S. Trans resveratrol loaded DSPE PEG 2000 coated liposomes: an evidence for prolonged systemic circulation and passive brain targeting. *J Drug Deliv Sci Technol*. 2016;33:125–135. doi:10.1016/j.jddst.2016.02.009
44. Roy B, Guha P, Bhattarai R, et al. Influence of lipid composition, pH, and temperature on physicochemical properties of liposomes with curcumin as model drug. *J Oleo Sci*. 2016;65:399–411. doi:10.5650/jos.ess15228
45. Reddy JA, Low PS. Enhanced folate receptor mediated gene therapy using a novel pH-sensitive lipid formulation. *J Control Release*. 2000;64:27–37. doi:10.1016/S0168-3659(99)00135-2
46. Shi G, Guo W, Stephenson SM, Lee RJ. Efficient intracellular drug and gene delivery using folate receptor-targeted pH-sensitive liposomes composed of cationic/anionic lipid combinations. *J Control Release*. 2002;80:309–319. doi:10.1016/S0168-3659(02)00017-2
47. Poh S, Chelvam V, Ayala-López W, Putt KS, Low PS. Selective liposome targeting of folate receptor positive immune cells in inflammatory diseases. *Nanomedicine*. 2018;14:1033–1043. doi:10.1016/j.nano.2018.01.009
48. Li Q, Rao R, Vazzana J, et al. Regulating mammalian target of rapamycin to tune vaccination-induced CD8(+) T cell responses for tumor immunity. *J Immunol*. 2012;188:3080–3087. doi:10.4049/jimmunol.1103365
49. Shor B, Gibbons JJ, Abraham RT, Yu K. Targeting mTOR globally in cancer: thinking beyond rapamycin. *Cell Cycle*. 2009;8:3831–3837. doi:10.4161/cc.8.23.10070
50. Sabatini DM. mTOR and cancer: insights into a complex relationship. *Nat Rev Cancer*. 2006;6:729–734. doi:10.1038/nrc1974
51. Guertin DA, Sabatini DM. Defining the role of mTOR in cancer. *Cancer Cell*. 2007;12:9–22. doi:10.1016/j.ccr.2007.05.008
52. Chiang GG, Abraham RT. Phosphorylation of Mammalian Target of Rapamycin (mTOR) at ser-2448 is mediated by p70S6 kinase. *J Biol Chem*. 2005;280:25485–25490. doi:10.1074/jbc.M501707200
53. Hardie DG. AMP-activated protein kinase: an energy sensor that regulates all aspects of cell function. *Genes Dev*. 2011;25:1895–1908. doi:10.1101/gad.17420111
54. Wang W, Guan KL. AMP-activated protein kinase and cancer. *Acta Physiologica*. 2009;196:55–63. doi:10.1111/j.1748-1716.2009.01980.x
55. Kim J, Kundu M, Viollet B, Guan KL. AMPK and mTOR regulate autophagy through direct phosphorylation of Ulk1. *Nat Cell Biol*. 2011;13:132. doi:10.1038/ncb2152
56. Egan DF, Shackelford DB, Mihaylova MM, et al. Phosphorylation of ULK1 (hATG1) by AMP-activated protein kinase connects energy sensing to mitophagy. *Science*. 2011;331:456–461. doi:10.1126/science.1196371

57. Wirth M, Joachim J, Tooze SA. Autophagosome formation–the role of ULK1 and Beclin1-PI3KC3 complexes in setting the stage. *Semin Cancer Biol*. 2013;23:301–309. doi:10.1016/j.semcancer.2013.05.007
58. Schmelzle T, Hall MN. TOR, a central controller of cell growth. *Cell*. 2000;103:256–262. doi:10.1016/S0092-8674(00)00117-3
59. Kirkin V, Lamark T, Sou Y-S, et al. A role for NBR1 in autophagosomal degradation of ubiquitinated substrates. *Mol Cell*. 2009;33:505–516. doi:10.1016/j.molcel.2009.01.020
60. Caramés B, Hasegawa A, Taniguchi N, Miyaki S, Blanco FJ, Lotz M. Autophagy activation by rapamycin reduces severity of experimental osteoarthritis. *Ann Rheum Dis*. 2012;71:575–581. doi:10.1136/annrheumdis-2011-200557
61. Redelman-Sidi G, Glickman MS 1, Bochner BH. The mechanism of action of BCG therapy for bladder cancer–a current perspective. *Nat Rev Urol*. 2014;11:153–162. doi:10.1038/nrurol.2014.15
62. Nie S, Hsiao WL, Pan W, Yang Z. Thermoreversible Pluronic F127-based hydrogel containing liposomes for the controlled delivery of paclitaxel: in vitro drug release, cell cytotoxicity, and uptake studies. *Int J Nanomedicine*. 2011;6:151–166. doi:10.2147/IJN.S25646
63. Matanović MR, Kristl J, Grabnar PA. Thermoresponsive polymers: insights into decisive hydrogel characteristics, mechanisms of gelation, and promising biomedical applications. *Int J Pharm*. 2014;472:262–275. doi:10.1016/j.ijpharm.2014.06.029
64. Kristl J, Pecar S, Smid-Korbar J, Schara M. Molecular motion of drugs in hydrocolloids measured by electron paramagnetic resonance. *Pharm Res*. 1991;8:505–507.

Supplementary materials

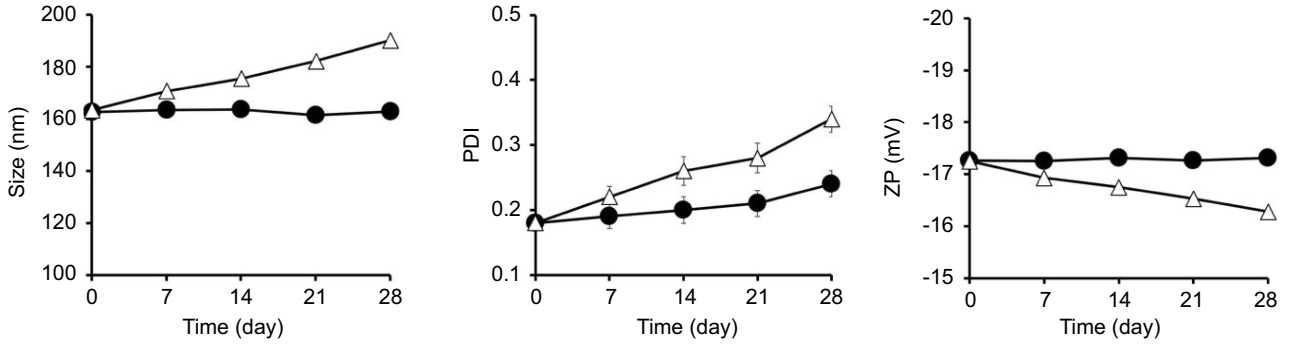

Figure S1 Stability evaluation of R-CL during storage at 4 °C (●) and 25 °C (△) for 4 weeks.
Notes: Data represent the means ± SD (n=3).
Abbreviations: PDI, polydispersity index; ZP, zeta potential.

Table S1 Composition and physical characteristics of prepared liposomes

	DiI-loaded liposomes	
	CL	**FL**
Composition (mol ratio)		
SPC	90	89.5
Cholesterol	10	10
$DP_{2K}F$	–	0.5
DiI (added)	10	10
Physical properties		
Size (nm)	156.3±0.32	156.7±0.63
PDI	0.16±0.04	0.14±0.03
ZP (mV)	−7.48±0.59	−16.25±0.48
EE (%)	44.5±0.32	44.2±0.27

Notes: Values represent the mean ± SD (n=3).
Abbreviations: CL, conventional liposome; FL, folate-modified liposome; SPC, soy phosphatidylcholine; $DP_{2K}F$, distearoylphosphatidylethanolamine-polyethylene $glycol_{2000}$-folate; DiI, 1,1′-dioctadecyl-3,3,3′,3′-tetramethylindocarbocyanine perchlorate; PDI, polydispersity index; ZP, zeta potential; EE, entrapment efficiency.